Acoustic dispersion in a ball-shaped surface acoustic wave device

doi: 10.1063/1.2741606

Acoustic dispersion in a ball-shaped surface acoustic wave device

Kazushi Yamanaka,[a),b)] Kanwar Jit Singh,[c)] Naoya Iwata,[a)] and Takuji Abe[a)]
Tohoku University, Aoba 02, Sendai, Miyagi 980-8579, Japan

Shingo Akao, Yusuke Tsukahara, and Noritaka Nakaso
Toppan Printing Co., Ltd., Sugito, Kitakatsushika-gun, Saitama 345-8508, Japan

(Received 25 March 2007; accepted 27 April 2007; published online 24 May 2007)

Theoretical model for ball surface acoustic wave (SAW) sensors has been developed. Wave front distortion encountered in planar SAW sensors caused by diffraction or reflection can be neglected because of the diffraction-free propagation of a naturally collimated beam. Wave form at each turn is expressed by an integral of terms defined by the array factor and the elementary charge density of electrodes as well as the frequency-dependent velocity and attenuation caused by the sensitive film. Irrespective of the significant simplicity of the theory, excellent agreement has been observed between the simulated and experimental wave forms of a double-electrode ball SAW sensor.
 [DOI: 10.1063/1.2741606]

Diffraction[1] takes place when waves of finite width propagate. This phenomenon leads to the decrease in the total wave energy within the source aperture causing diffraction loss. Surface acoustic waves[2,3] (SAWs) are also attenuated by diffraction loss, posing a limitation on the performance of SAW devices. However, SAWs on a ball (sphere)[4–10] have distinct character. In particular, a naturally collimated beam is formed[6–9] when the aperture width is approximately equal to the square root of the product of the wavelength and diameter due to the balance between the effects of diffraction and focusing.[11,12] This greatly reduces the SAW attenuation since the beam is not disturbed by supports, defects, or nonuniformities outside the narrow collimated beam. On the basis of this advantage, a ball SAW sensor has been proposed[13–15] and verified in hydrogen-sensing experiments.[15,16] Nevertheless, its performance is largely influenced by the configuration of the interdigital transducer[17] (IDT) and the sensitive film. During optimizing these devices, the calculation of wave forms with and without a sensitive film is essential, although precise calculation for an anisotropic crystal sphere is extremely difficult.

In this work, a simple theory for the calculation of complex roundtrip wave forms was developed, taking advantage of the wave front preservation of the diffraction-free propagation of a collimated beam. The wave front distortion caused by diffraction or reflection was neglected. During comparison with measured wave forms, we found that the theory is sufficiently precise if the alignment error of the IDT is small. In complex-shaped wave forms of a double-electrode device used for temperature compensation, the superposition of fundamental and third harmonic components was reproduced with high precision.

Formulation of the theoretical model which may generate analogous acoustic signals as obtained by the experimental ball SAW sensor would help to understand the physics of SAW propagation and interaction with gas in a better way.

Figure 1 shows the ball SAW device. If a SAW on a ball is collimated, the wave form after an arbitrary number (n) of turns has a shape identical to that of the first turn since it is not influenced by reflection or diffraction. Thus, the wave form after n turns is expressed as $s_n(t)=\exp[i\omega(t-nL/V_P)]\exp[-\alpha nL]$, where $L=2\pi r$ is the circumference of the ball with the radius r, V_P is the phase velocity, and α is the attenuation coefficient per unit length (1/m) of the SAW on the ball. If the material is anisotropic, the validity of this equation is not self-evident. However, it can be justified if the appropriate crystallographic orientation is satisfied with respect to the roundtrip routes. In fact, wave forms with almost single exponential decay with higher Q factor (>40 000) have been experimentally observed in the Z-cylinder route of a quartz ball.[14,15] Further justification will be given later by showing that the theory based on this equation can precisely reproduce experimentally observed wave forms.

The effect of acoustic dispersion on the SAW pulse shape can be obtained with the help of the Fourier integral theorem as $s(t)=1/(2\pi)\int_{-\infty}^{\infty}S(\omega)\exp(i\omega t)d\omega$ with $S(\omega)=\int_{-\infty}^{\infty}s(t)\exp(-i\omega t)dt$, where $S(\omega)$ is the Fourier transform of the input signal with $\omega(=2\pi f)$ as the angular frequency. For a short tone burst in a ball SAW device, we propose the following expression, modifying the previous expression for the continuous wave:[13]

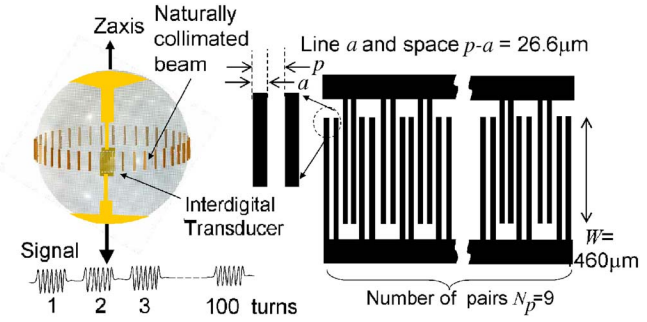

FIG. 1. (Color online) Ball SAW device with diffraction-free propagation of naturally collimated SAW beam and a double-electrode IDT for two frequency generation.

[a)]Also at: JST-CREST, 4-1-8 Hon-chou, Kawaguchi, Saitama 332-0012, Japan.
[b)]Electronic mail: yamanaka@material.tohoku.ac.jp
[c)]On leave from: Applied Physics Department, Guru Nanak Dev University, India.

TABLE I. Parameters used to simulate the wave forms with common values for the cases A and B: bandwidth $\Delta\omega/2\pi=30.0$ MHz, center wavelength $2\pi/k_0=212.8$ μm, number of electrode pairs $N_p=9$, circumference of the ball $L=0.0314$ m, and SAW velocity at zero frequency $V_R=3209$ m/s.

Sensitive film	Center frequency $\omega_0/2\pi$ (MHz)	Velocity dispersion parameter$c$ (m^2/s)	Q factor
A (without film)	14.5	0	5.5×10^4
B (with film)	14.6	−169.3	4.4×10^4

$$s_O(t)=\frac{C}{2\pi}\sum_{n=1}^{N}\int_{k_0-\Delta k}^{k_0+\Delta k}|A(k)\rho_f(k)|^2S[\omega(k)]\exp\left[i\omega(k)\left(t-\frac{nL}{V_P(k)}\right)\right]\exp[-\alpha(k)nL]\frac{\partial\omega}{\partial k}dk, \quad (1)$$

where the time range is defined as $nL/V_{G1}\leqslant t<(n+1)L/V_{G2}$ for each n, $A(k)$ is the array factor, $\rho_f(k)$ is the elemental charge density, C is a constant representing the electrode structure and electromechanical coupling, k is the wave number, $k_0=2\pi/\lambda$ is the center wave number determined by the period of the electrodes, Δk is the effective width of the wave number spectrum, and V_{G1} and V_{G2} are the smallest and largest group velocities of the SAW in the range of $k=k_0\pm\Delta k$, respectively, which can be approximated by the Rayleigh wave velocity of the substrate V_R when the velocity dispersion is not significant. For the input signal of a tone burst with a Gaussian envelope,

$$s(t)=\left(\frac{\Delta\omega^2}{2\pi}\right)^{1/4}\exp(i\omega t-\Delta\omega^2t^2/4),$$

$$S(\omega)=\left(\frac{2}{\pi\Delta\omega^2}\right)^{1/4}\exp\left(-\left[\frac{(\omega-\omega_0)}{\Delta\omega}\right]^2\right), \quad (2)$$

where ω_0 and $\Delta\omega$ are the center frequency $\Delta\omega$ and the bandwidth of the electrical circuits for transmission and reception, respectively. Although they can be rigorously defined, they will be used in this letter as adjustable parameters for comparison with experimental results (Table I).

The elemental charge density is given by

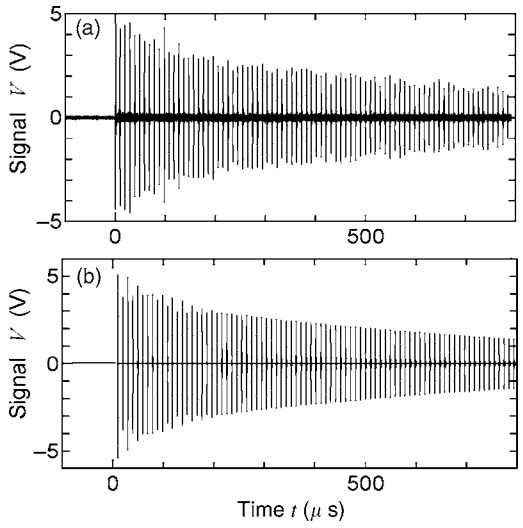

FIG. 2. (a) Measured wave form and (b) calculated wave form for multiple roundtrips of 80 turns with the 40 nm PdNi film.

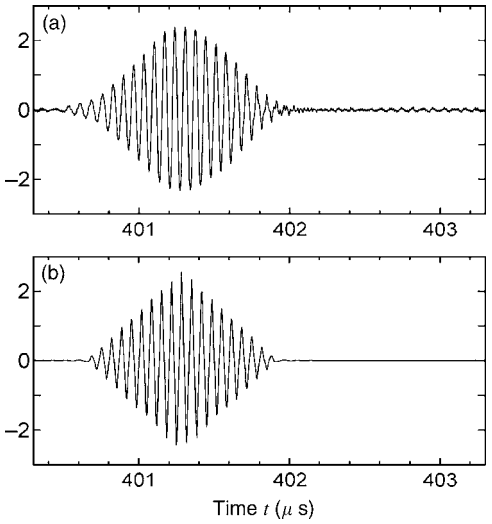

FIG. 3. (a) Experimental wave form and (b) calculated wave form at 39th turn without the film. The parameters used for calculation are given in Table I.

$$\rho_f(k)=2(\varepsilon_0+\varepsilon_p)\sin(\pi s)/[P_{-S}(-\cos\Delta)]P_m(\cos\Delta), \quad (3)$$

for $m\leqslant kp/(2\pi)\leqslant m+1$ $(m=0,1,2)$, where ε_0 is the permittivity of the vacuum, ε_p is a function of the permittivity components of the material,[17] $\Delta=\pi a/p$, $S=kp/(2\pi)-m$, $P_{-S}(-\cos\Delta)$ is a Legendre function, $P_m(\cos\Delta)$ is a Legendre polynomial, $p=\lambda/2$ is the period of the double electrode, and a is the width of the electrode. The array factor for the double-electrode transducers, as shown in Fig. 1, is

$$A(k)=2[\sin(2N_Pkp)/\sin(2kp)]\cos(kp/2), \quad (4)$$

where N_P is the number of electrode pairs. If the metallization ratio is $a/p=1/2$, only the fundamental wave and third harmonics are generated, and the fifth and seventh harmonics are suppressed by the effect of the elemental charge density, given by Eq. (3).[17]

The dispersion relation $\omega=\omega(k)$ is given for the sensitive film as $\omega=V_Rk+(c/2)k^2$, which gives phase and group velocities of $V_P=\omega/k=V_R+(c/2)k$ and $V_G=\partial\omega/\partial k=V_R+ck$, respectively. Here, c is the velocity dispersion parameter.

The group velocity changes from V_R at dc to V_R+ck_0 at the center wave number $k=k_0$ with the variation $\Delta V(=ck_0)$. The attenuation is given by $\alpha=\omega/(2QV_R)$ (1/m), where $Q=\pi f/(V_R\alpha)=\pi f/\alpha_t$ is the quality factor and α_t is the attenuation per unit time (1/s). If Q is constant, the attenuation is proportional to the frequency. Substitution of Eqs. (2)–(4) in eq. (1) gives the wave form.

A 10-mm-diameter quartz ball with a double-electrode IDT was fabricated.[16] PdNi film was thermally evaporated under a pressure of 10^{-4} Pa with a thickness of 40 nm and about 85% of the Z-axis cylinder route[14] was covered with the film to sense H_2.[15] The input signals were generated using a broadband pulser. Impulse signals with a width of 2 ns were input to the double-electrode IDT(Ref. 17) fabricated on the equator of a 10-mm-diameter single-crystal quartz ball.[14]

Figure 2(a) shows the measured wave form for multiple roundtrips of 80 turns with the PdNi film. The group velocity at zero frequency was obtained from the average separation of peaks for each turn of a similar sensor. For example, the velocity of the sensor without the film was estimated from

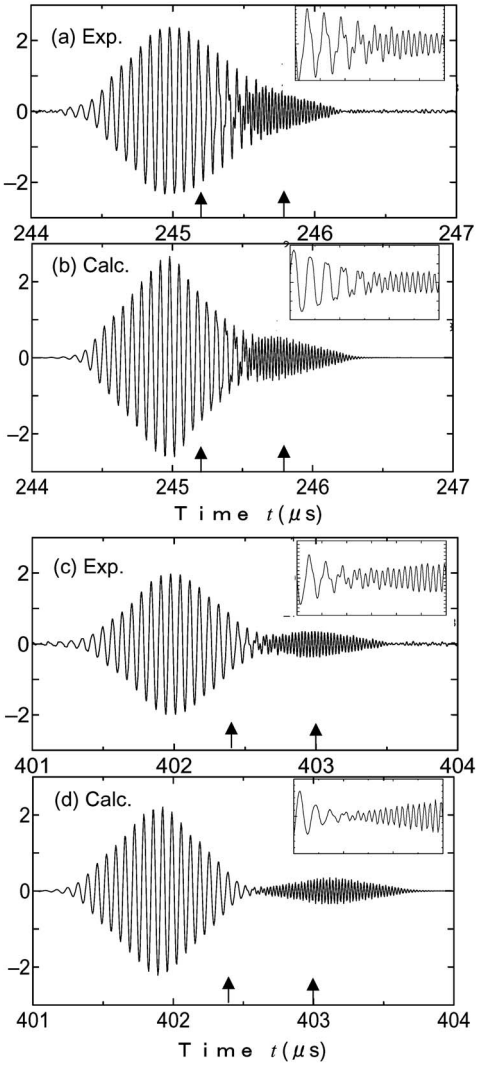

FIG. 4. (a) Experimental wave form and (b) calculated wave form at 24th turn with the 40 nm PdNi film. (c) Experimental wave form and (d) calculated wave form at 39th turn with the 40 nm PdNi film. The parameters used for calculation are given in Table I. The arrows indicate horizontal axis range of the insets.

the average roundtrip time of 9.79 μs and the circumference of 10π mm to be $=10\pi/9.79=3209$ m/s, as listed in Table I. The Q factor was obtained from log plots of the amplitudes of 15 and 45 MHz components of the signal at each turn, evaluated by the root mean square of the wave forms after frequency filtering by fast Fourier transform. The logarithm of the amplitude linearly decreased as a function of the propagation distance. From the slope, the attenuation coefficients α and Q were obtained, as shown in Table I.

Experimental wave form at the 39th turn without the film is shown in Fig. 3(a). Figures 4(a) and 4(c) show the wave forms at the 24th and 39th turns with the film. It is noted that the third harmonics propagate more slowly than the fundamental wave due to the velocity dispersion caused by the film. The dispersion parameter c was obtained by analysis of the data in Figs. 4(a) and 4(c) and is shown in Table I. The array factor and spectrum of an input tone burst with a Gaussian envelope were obtained from the ball SAW device with the design, as shown in Fig. 1. These parameters are listed in Table I.

Wave forms were calculated using Eqs. (3)–(6) and the parameters in Table I. Figure 2(b) shows the calculated wave form for multiple roundtrips of 80 turns with the film. The irregular variation of the amplitude observed in the time range of 0–200 μs is caused by the interference of the two frequency components with different phase velocities.

The calculated wave form at the 39th turn without the film is shown in Fig. 3(b); the position, number of carriers, and shape of the envelope are similar to those of the measured wave form in Fig. 3(a). Similarly, the calculated wave forms at the 24th and 39th turns with the film are shown in Figs. 4(b) and 4(d); the position, number of carriers, and shape of the envelope are again similar to those of the experimental wave forms in Figs. 4(a) and 4(c). In contrast to the case without the film, third harmonic components were also well reproduced, localized in the later part of the wave form because of the velocity dispersion. The transition from the fundamental frequency to the third harmonic frequency at around 245 μs, as shown in the insets of Figs. 4(a) and 4(c), was also reproduced in Figs. 4(b) and 4(d). The agreement between the experimental and calculated wave forms is excellent, irrespective of the complexity of the wave forms and the simplicity of the theory. The excellent precision of the theory is based on the fundamental property of the ball SAW device, i.e., the wave front preservation due to the diffraction-free propagation of a naturally collimated beam.[6–11]

Helpful discussions with Professor Ken-ya Hashimoto, Chiba University, are greatly appreciated.

[1]M. Born and E. Wolf, *Principles of Optics*, 7th ed. (Cambridge University Press, Cambridge, UK, 1999), pp. 412–426.
[2]J. D. N. Cheeke, *Fundamentals and Applications of Ultrasonic Waves* (CRC, Boca Raton, London, 2002), p. 87.
[3]K. Hashimoto, Jpn. J. Appl. Phys., Part 1 **45**, 4423 (2006).
[4]I. A. Viktrov, *Rayleigh and Lamb Waves* (Plenum, New York, 1967), p. 42.
[5]D. Royer, E. Dieulesaint, X. Jia, and Y. Shui, Appl. Phys. Lett. **52**, 706 (1988).
[6]K. Yamanaka, H. Cho, and Y. Tsukahara, Appl. Phys. Lett. **76**, 2797 (2000).
[7]K. Yamanaka, H. Cho, and Y. Tsukahara, Institute of Electronics, Information and Communication Engineers Technical Report No. US2000–14, 49 (2000).
[8]S. Ishikawa, Y. Tsukahara, N. Nakaso, H. Cho, and K. Yamanaka, Jpn. J. Appl. Phys., Part 1 **40**, 3623 (2001).
[9]Y. Tsukahara, N. Nakaso, H. Cho, and K. Yamanaka, Appl. Phys. Lett. **77**, 2926 (2000).
[10]S. Ishikawa, H. Cho, N. Nakaso, Y. Tsukahara, and K. Yamanaka, Ultrasonics **41**, 1 (2003).
[11]S. Ishikawa, N. Nakaso, N. Takeda, D. Y. Sim, T. Mihara, Y. Tsukahara, and K. Yamanaka, Appl. Phys. Lett. **83**, 4649 (2003).
[12]D. Clorennec and D. Royer, Appl. Phys. Lett. **85**, 2435 (2004).
[13]Y. Tsukahara, N. Nakaso, H. Cho, and K. Yamanaka, Institute of Electronics, Information and Communication Engineers Technical Report No. US2000–55, 31 (2000).
[14]N. Nakaso, Y. Tsukahara, S. Ishikakwa, and K. Yamanaka, Proc.-IEEE Ultrason. Symp., 47 (2002).
[15]K. Yamanaka, S. Ishikawa, N. Nakaso, N. Takeda, D. Y. Sim, T. Mihara, A. Mizukami, I. Satoh, S. Akao, and Y. Tsukahara, IEEE Trans. Ultrason. Ferroelectr. Freq. Control **53**, 793 (2006).
[16]T. Nakatsukasa, S. Akao, T. Ohgi, N. Nakaso, T. Abe, and K. Yamanaka, Jpn. J. Appl. Phys., Part 1 **45**, 4500 (2006).
[17]D. Morgan, *Surface-Wave for Signal Processing* (Elsevier, Amsterdam, The Netherlands, 1991), p. 59.